

Summer 2012

Thermal Modeling of Nanosat

Dai Dinh

San Jose State University

Follow this and additional works at: http://scholarworks.sjsu.edu/etd_theses

Recommended Citation

Dinh, Dai, "Thermal Modeling of Nanosat" (2012). *Master's Theses*. 4193.
http://scholarworks.sjsu.edu/etd_theses/4193

This Thesis is brought to you for free and open access by the Master's Theses and Graduate Research at SJSU ScholarWorks. It has been accepted for inclusion in Master's Theses by an authorized administrator of SJSU ScholarWorks. For more information, please contact scholarworks@sjsu.edu.

THERMAL MODELING OF NANOSAT

A Thesis

Presented to

The Faculty of the Department of Mechanical and Aerospace Engineering

San José State University

In Partial Fulfillment

of the Requirements for the Degree

Master of Science

by

Dai Q. Dinh

August 2012

© 2012

Dai Q. Dinh

ALL RIGHTS RESERVED

The Designated Thesis Committee Approves the Thesis Titled

THERMAL MODELING OF NANOSAT

by

Dai Q. Dinh

APPROVED FOR THE DEPARTMENT OF MECHANICAL AND AEROSPACE
ENGINEERING

SAN JOSE STATE UNIVERSITY

August 2012

Dr. Periklis Papadopoulos Department of Mechanical and Aerospace Engineering

Dr. Marcus Murbach NASA Ames Research Center

Dr. Sean Swei Department of Mechanical and Aerospace Engineering

ABSTRACT

THERMAL MODELING OF NANOSAT

by Dai Q. Dinh

Miniaturization of electronic components enabled small scale satellite projects, such as the CubeSat, to be used for scientific research in space. Recently a team of undergraduate and graduate students at San Jose State University (SJSU) had the opportunity to collaborate on designing and building a miniature size CubeSat with the dimensions of $10 \times 10 \times 10 \text{ cm}^3$. Although the integration of compact electronics allowed sophisticated scientific experiments and missions to be carried out in space, the thermal control options for such small spacecraft were limited. For example, due to the CubeSat's small size there was no room for dedicated a radiator or insulation panels. To minimize mass of the thermal control system while keeping the electronics at safe operating conditions, this thesis research was designed to study the external orbital radiation heat flux the CubeSat would be expected to be exposed to and the steady state heat conduction of the internal electronics. Numerical simulation and analytical results showed that the operating temperatures of the electronics were within the safety limits.

ACKNOWLEDGEMENTS

I would first like to thank my thesis advisor, Dr. Periklis Papadopoulos, for all his help and guidance over many years in shaping my education, especially for helping getting through this thesis. Dr. Papadopoulos, I thank you for your kindness and for all the time that you have spent helping me. The material contained in this thesis wouldn't have been possible without your guidance.

I would also like to thank Dr. Nikos Mourtos, Dr. Sean Swei and Dr. Marcus Murbach for being the committee members of this thesis. Dr. Mourtos' lectures on Aerodynamics and Dr. Swei's lectures on Aircraft Control and Stability have helped shaped my education.

Finally I would like to thank my mom and all my friends and colleagues for all the support and encouragement. I would also like to thank all students working on the CubeSat project for providing helpful information for this thesis.

Table of Contents

List of Figures	viii
List of Tables	ix
Chapter 1 Introduction	1
1.1 Introduction to CubeSat	1
1.2 Motivations.....	4
1.3 Objectives.....	4
Chapter 2 Theoretical Background	7
2.1 Heat Transfer.....	7
2.1.1 Conduction Heat Transfer	8
2.1.2 Radiation Heat Transfer.....	9
2.2 Space Thermal Environment.....	10
2.3 Orbital Mechanics	14
Chapter 3 CubeSat System Design and Power Budget Analysis.....	21
3.1 Subsystems Overview	21
3.2 Attitude Control Subsystem	22
3.3 Structural Subsystem.....	22
3.4 Communication Subsystems	23
3.5 Power and Electrical Subsystems (EPS)	23
Chapter 4 Thermal Modeling Approach	25
4.1 External Analysis Approach.....	25
4.2 Internal Analysis Approach.....	26
Chapter 5 Thermal Modeling Results and Discussion.....	31
5.1 External Analysis with Thermal Desktop	31
5.2 Internal Simulation with Ansys Icepak	33
Chapter 6 Design of Experiments Simulation	38
Chapter 7 Conclusions and Future Work.....	41
References.....	44

APPENDIX A – STK Setup	45
APPENDIX B – Thermal Desktop Setup Guide	46

List of Figures:

Figure 1-1 CubeSat Model.....	3
Figure 2-1 Space Thermal Environment for CubeSat.....	12
Figure 2-2 Beta Angle.....	15
Figure 2-3 Orbital Parameters for Low Earth Orbit.....	16
Figure 2-4 Thermal Desktop Orbit Input Options	17
Figure 2-5(a) CubeSat Orbit for Beta Angle = 90°. (b) Beta Angle = 30°.	18
Figure 2-6 CubeSat Lifetime– Apogee, Perigee and Eccentricity Variation.....	19
Figure 3-1 Example of a CubeSat Model – Exploded View	21
Figure 4-1 BeagleBoard Top Side Components	28
Figure 4-2 BeagleBoard Heat Conduction.....	29
Figure 4-3 1.2 W Power Dissipation through CU Block Under Natural Convection.....	30
Figure 5-1 External Heating at 400 km Altitude	31
Figure 5-2 External Heat Flux	32
Figure 5-3 Total Absorbed Heat Flux for 400 km Altitude	33
Figure 5-4 CubeSat Temperature Profile – Hot Case Analysis	35
Figure 5-5 CubeSat Temperature Profile – Cold Case Analysis	36
Figure 6-1 CubeSat Total Absorbed Flux.....	38
Figure 6-2 Total Absorbed Heat Flux for Beta Angle = 90°.....	39
Figure 6-3 Total Absorbed Heat Flux for Beta Angle = 30°.....	40
Figure A-1 Satellite Orbit Setup in STK.....	45
Figure A-2 CubeSat Lifetime – Apogee, Perigee and Eccentricity Variation	45

List of Tables:

Table 2-1 LEO Thermal Environment (Adapted from [5], [7] and [9])	11
Table 3-1 Power Budget for CubeSat	24
Table 4-1 Optical Properties	26
Table 4-2 Thermal Physical Properties	28
Table 5-1 Component Temperatures	37

Chapter 1

Introduction

1.1 Introduction to CubeSat

Advances in computer technologies and manufacturing processes allow the creation of highly sophisticated components within a compact platform. This miniaturization of components allow small scale satellites, such as the CubeSat, to be used for scientific research in space rather than a large scale project like the International Space Station (ISS). The CubeSat concept was originally developed in 1999 by Dr. Jordi Puig-Suari from the California Polytechnic State University and Professor Bob Twiggs from the Stanford University [1]. The goal of the CubeSat project was to reduce development time and to increase launch opportunity through standardized satellite buses, structures, and subsystems. This allows academia and commercial entities to perform space research at affordable price. This also creates opportunities for many undergraduate and graduate students to have hands-on experience building small payload satellite that can be launch to space as a secondary payload. A CubeSat is typically a 10 cm³ made of aluminum T6061 structure with a total mass of up to 1 kg and operates autonomously in orbit. This small satellite design model can easily be modified to accommodate different missions. Since its invention the project has grown into an international collaboration project of over 40 universities, high schools, and private firms. Under the coordination of the California Polytechnic State University at San Luis Obispo, 14 CubeSats were successfully launched using the standardize Poly-PicoSatellite Orbital

Deployer (P-POD) on March 2005 using the Dnepr launch vehicle [1]. Another international collaboration project, called QB50, to put 50 CubeSats for multi-point, in-situ measurements in the lower thermosphere, is also in development with a target launch date in 2014 [2].

Many students at San Jose State University (SJSU) had the opportunity to work on CubeSat in 2009 with Bob Twiggs, who was one of the pioneer creators of the CubeSat project. With appropriate funding, the aerospace engineering undergraduate students built the several versions of the CubeSat for their senior projects. However, because of the limited time available for the students to work on the project, most of the CubeSats were built without numerical modeling or experimental testing because the satellite is assumed to function as designed. The objective of this thesis was to perform numerical thermal modeling of a general CubeSat using different commercial applications. Thermal Desktop was used to model the external orbital heating rate. The result obtained from this analysis was then used as the wall boundary condition for the internal thermal analysis in Ansys Icepak.

There are three main operating phases concerning the thermal environment of the CubeSat are (1) launch, (2) mission lifetime, and (3) reentry self-destruction. The purpose of this thesis was to perform a detailed analysis of the CubeSat in phase 2, the mission lifetime in orbit. Typically the CubeSats are deployed on a standard flight-proven Poly Picosatellite Orbital Deployer (P-POD) deployment system from CalPoly without further analysis except for qualitative tests to ensure mission safety. The

assumption is that the CubeSat is safe inside the P-POD for transport and launch.

Without a proper thermal protection system for reentry, the CubeSats are designed to be burned up in the atmosphere during reentry. Alternatively the CubeSat can be picked up by a larger satellite. Therefore phase 1 and phase 3 were not considered in this thermal analysis. It was the goal of this thesis to make sure the system was operating within safety limit by performing thermal simulation of the CubeSat to study the internal heat conduction and the external heat radiation.

A typical CubeSat consists of an anodized aluminum structure with space inside for mounting the hardware. Figure 1-1 showed an example of the 3-D CAD model of a CubeSat. Depending on the mission objective, there are usually several levels of embedded hardware with different power consumption. Details information on CubeSat subsystems are further discussed in Chapter 3.

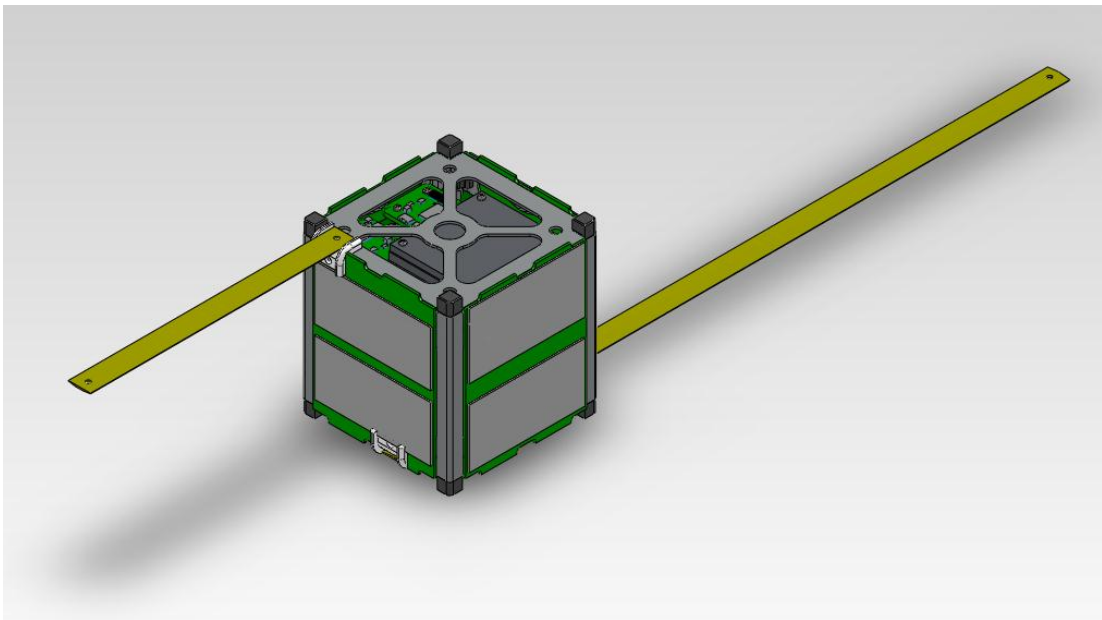


Figure 1-1 CubeSat Model

1.2 Motivations

A group of undergraduate and graduate students in aerospace engineering at San Jose State University collaborated to analyze, design and build a CubeSat with the purpose of testing communication and tracking modules as a technological demonstration. Although the design and assembly of the satellite were completed, detailed analysis was not yet performed. This created the opportunity for graduate students to perform detailed analysis on various aspects of the design such as structural and vibrational analysis, and power system design and thermal analysis. The motivation for this thesis was to perform detailed system-level thermal analysis of the CubeSat in Low Earth Orbit (LEO) at 400 km altitude to verify numerically that all electrical components were operating within the thermal design limits. This thesis also explored different design configurations to make sure the satellite will be able to operate safely in its environment for future missions.

1.3 Objectives

With the opportunity to build flight hardware with real access to space as a secondary payload, many educational institutions have been building the CubeSat with different mission objectives [1]. The missions can range from measuring the temperature in the thermosphere to experimenting and validating different communication systems for future nano- and pico-satellite missions.

The thermal subsystem of a satellite depends on various parameters such as the geometry, structure, and onboard electronic components. For small scale satellite like the CubeSat, the thermal control option was limited and often resorted to passive devices. To ensure components operability and mission success, a thermal analysis, either through numerical or experimental methods, was necessary to benchmark against components temperature limits. When the operating temperatures exceeded the specified limits, different approaches were investigated to achieve proper thermal control.

The objective of this thesis was to perform thermal simulation of the CubeSat using Thermal Desktop and ANSYS Icepak to make sure that the internal electronics were operating within the various specified safety limits. The goal was to demonstrate numerical simulations could be used to predict and optimize the temperature distribution of the space system before it was built. Electronics operating temperature typically range from -25 to 85°C, solar panels range from -85 to 100°C, and batteries range from -40° to 60°C [3]. At any given time the CubeSat would have at most three faces facing the sun, while the other faces were in the shadow facing and absorbing the earth's albedo. If the electronics were not operating within safety range during flight operation, either active or passive thermal control, such as heater, isolator, heat pipes, or louvers, would be used. Alternatively the CubeSat could be set into hibernation until it got to a certain orbit position that would allow all the components to operate at within the safety limits. The analysis would include both internal heat transfer conduction and an external radiation analysis. At 400 km mission altitude and with the beta angle of 56 degrees, the CubeSat would spend about 65 minutes exposing to the sun, and about 35 minutes in the eclipse

region for each orbital period. The steady state analyses were divided into two cases (1) “hot case” for facing the sun and (2) “cold case” for the satellite during eclipse.

Chapter 2

Theoretical Background

2.1 Heat Transfer

When the electrical current flows through the electronic devices to power the system, a portion of the power generates heat as a by-product of normal operation. Sometimes excess in generated heat could damage the device, which makes proper thermal management and thermal analysis a necessity to ensure device operability and reliability. Heat is typically transfers in three ways (1) convection, (2) conduction, and (3) radiation. However, since the density of air at very high altitudes is extremely low from the Low Earth Orbit (LEO) and beyond, the available air for natural cooling is negligible. Space heat transfer is then predominately control by conduction and radiation. Without natural convection to cool off the electronics, a system operating at the same power input in space is more likely to result in a higher temperature compared to that operating at sea level.

For space applications, the heat on the external of the spacecraft mainly comes from direct solar radiation from the sun. In general, when the CubeSat was tilted relatively to the sun, the solar flux could “see” at most three faces. The worst case scenario, in terms of heat transfer, was when one side of the CubeSat faced directly to the sun and all the energy was either absorbed or reflected. This caused one side to be too hot, while the remaining five sides stayed cool. When the thermal analysis for future mission showed that the concentrated heat on one side was too high, passive thermal control solutions, such as heat pipes, were used to redirect the heat from the hot side to

the cold side. In addition to conduction and radiation, the CubeSat spins as it orbits the earth. This spinning effect, according to Gadalla [4], reduces the overall temperature on the external body. The primary goal of this thesis was to analyze the CubeSat thermal condition to ensure mission success, as well as to explore different design methods to keep the temperatures of the electronics within the specified operating temperature limits. A well-design system would incorporate passive or active cooling mechanisms, such as using thermal electric cooler (TEC) or heat pipes, to distribute the heat. The purposes of this thesis were to analyze thermal conditions of the CubeSat in space and explore possibilities of improvement for future missions. This section provides basic theoretical background to heat transfer and space related information relevant to the thermal analysis of the CubeSat. It would explain basic equations for conduction and radiation modes of heat transfer from the Fundamentals of Heat and Mass Transfer book by Incropera et al [5]. Explanations regarding the space environment and orbital mechanics came from the Space Mission Analysis and Design handbook by Larson et al [6, 7].

2.1.1 Conduction Heat Transfer

Conduction is the process by which heat is transferred through the solid, liquid, or gas from a high energy source to a relatively lower energy source. Conduction heat transfer can occur within a material, or from two or more contacting bodies. It is governed by Fourier's Law as follow:

$$q_x'' = -k \frac{dT}{dx} \quad (2.1)$$

where Q is the heat flow rate (W), k is the thermal conductivity (W/mK) of the material, dT/dx is the temperature differential over the length. Unlike the convective heat transfer mode, the conduction resistance inside the solid does not change with altitude.

The thermal resistance is a measure of the resistance of heat flow between contacting bodies through the thermal interface material, such as thermal pads or adhesive bonding materials. Thermal resistance, often expressed as °C/W or K/W, is found by

$$\theta_{cond} = \frac{\Delta T}{q_x} = \frac{L}{kA_C} \quad (2.2)$$

where A_C is the cross-sectional area available for conduction. One can quickly calculate the expected operating temperature of the device if the ambient temperature, the thermal resistance and the power consumption are known. For example, if the thermal resistance of a die package is 2.5 °C/W, the ambient temperature is 25°C and the chip consumes 2 W of power, then the expected temperature of the device would be 30°C.

2.1.2 Radiation Heat Transfer

Radiation heat transfer occurs by radiating the heat between two or more surfaces through space by electromagnetic waves. It is dependent on the temperature and the coating of the radiating surface. The radiation heat transfer is governed by Stefan-Boltzmann's Law as follow:

$$E = \sigma T^4 \quad (2.3)$$

where σ is the Stefan-Boltzmann constant, $5.67 \times 10^{-8} \text{ W/m}^2\text{K}^4$.

The amount of energy transfer through radiation between two bodies having temperatures of T_1 and T_2 is found by

$$q_r = \varepsilon \sigma F_{1,2} A (T_1^4 - T_2^4) \quad (2.4)$$

where:

q_r = amount of heat transfer by radiation (W)

ε = emissivity of the radiation surface (reflective = 0, absorptive = 1)

$F_{1,2}$ is the shape factor between surface area of body 1 and body 2 (≤ 1.0)

Unless the difference temperature between two or more bodies is high, radiation heat transfer is often very low. For example, the radiation energy between the sun and the spacecraft was taken into consideration for the external analysis of the CubeSat. However, the radiation between the internal electronics could be neglected because the maximum heat dissipation was only a fraction of 1 W of power.

2.2 Space Thermal Environment

The performance and operational lifetime of space systems are strongly influenced by the near-Earth space and atmospheric environments. For the CubeSat launching from the International Space Station (ISS) at approximately 400 km altitude, the atmospheric pressure and drag were very small, and hence aerodynamic heating and convective heat transfer was negligible. There are three main sources of heat for general spacecraft systems operating in the near-Earth environment, which includes the radiated heat from the sun, the albedo (the reflection of solar radiation) and planetary heating from the Earth (black-body radiation of the Earth) [7, 8]. This section provides basic

information about the space environment and how it relates to the thermal simulation of the CubeSat.

Solar activity varies daily and its variation between the solar maxima and minima often dictates the design of the spacecraft. Most CubeSats, however, were designed to be in orbit for only a short period of time, and hence, the average solar flux over an extended period of time was sufficient for the radiation analysis. The solar flux used for this analysis was 0.874 W/in^2 (1354 W/m^2). Another source of radiation is the reflected sunlight off the Earth's surface, also called albedo. The average albedo of the earth is about 0.3. Table 2-1 [7] provides a summary of the range of Direct Solar, Reflected Solar (Albedo), and Planetary Infrared for the planet Earth. The thermal simulations were performed on two worse case scenarios: (1) "Hot Case" during direct sunlight and (2) "Cold Case" during eclipse. The values used for the "Hot Case" simulation were approximately the values in the "Mean" column, and the values used for the "Cold Case" were in the "Eclipse" column. From Table 2-1 it could be seen that the solar intensity at approximately 1 AU from the sun was about 1371 W/m^2 .

Table 2-1 LEO Thermal Environment (Adapted from [5], [7] and [9])

	Perihelion	Aphelion	Mean (Hot Case)	Eclipse (Cold Case)
Direct Solar	1414 W/m^2	1323 W/m^2	1371 W/m^2	0
Albedo (average)	0.30 ± 0.01	0.30 ± 0.01	0.30 ± 0.01	0.25
Planetary IR (average)	$234 \pm 7 \text{ W/m}^2$	$234 \pm 7 \text{ W/m}^2$	$234 \pm 7 \text{ W/m}^2$	220 W/m^2

An important parameter to consider when performing thermal analysis for the spacecraft and satellite is that space vehicle often spins as it orbits the earth. This spinning effect causes the vehicle to receive heat on one side and dissipate heat through the remaining sides. The combine effect of a rotating spacecraft and space solar heating causes the temperature variation on the external body, depending on the orbit and position of spacecraft relative to the sun [10]. The space thermal environment for a general spacecraft in the earth orbit is shown in Figure 2-1 below.

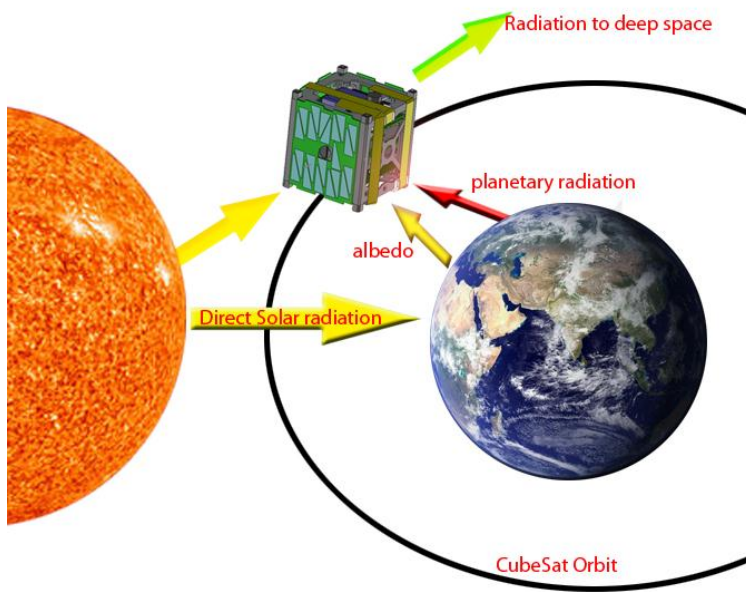


Figure 2-1 Space Thermal Environment for CubeSat

From a generalized heat balance equation for conservation of energy:

$$Q_{in} = Q_{out} \quad (2.5)$$

$$Q_{external} + Q_{internal} = Q_{radiated} \quad (2.6)$$

where $Q_{external}$ is the environmental heat absorbed, $Q_{internal}$ is the power dissipation by the internal electronics, and $Q_{radiated}$ is the heat rejected from the spacecraft to deep space.

Assuming the satellite is a black sphere, which means the absorptivity equals the reflectivity ($\alpha = \varepsilon = 1$), and that the satellite is in direct sunlight with the effect of planetary heating and albedo, the satellite energy balance for the hot case calculation can be shown as follows

$$A_{solar}q_s + FA_{surface}\sigma\bar{T}_E^4 + FA_{surface}aq_s + Q = A_{surface}\sigma\bar{T}^4 \quad (2.7)$$

where:

$$A_{surface} = 4\pi r^2, A_{solar} = A_{albedo} = A_{planetary} = \pi r^2,$$

F is the view factor ($F = 1/2$ for a spherical spacecraft assumption, and $F = 1/6$ for one side of the CubeSat (cube shape)), $a = 0.3$ is the Earth's albedo,

$Q = 0$ for internal heating.

Solving for the average surface temperature \bar{T} of the CubeSat, Equation (4.5) becomes

$$\bar{T}^4 = \frac{q_s}{\sigma} \left(\frac{1}{4} + Fa \right) + F\bar{T}_E^4 = \frac{1371}{5.67 * 10^{-8}} \left(\frac{1}{4} + 0.15 * 0.3 \right) + 0.15 * 255^4$$

For $q_s = 1371 \text{ W/m}^2$, $\sigma = 5.67 \times 10^{-8} \text{ W/m}^2\text{K}^4$, $F = 0.15$, $a = 0.3$, and $\bar{T}_E^4 = 255\text{K}$, the CubeSat equilibrium temperature is about 297 K or 24 °C. Similarly, when the satellite is

in eclipse, the term $A_{solar}q_s$ in Equation (2.7) becomes zero and the cold case calculation for the average surface temperature is about 198 K or -75 °C.

2.3 Orbital Mechanics

This section provides fundamental theory dealing with orbital mechanics to help aid the understanding of orbital heating simulation study. First, an important variable for this analysis is the beta angle, which determines the amount of time the spacecraft is exposing to direct sunlight. Beta angle is defined as the angle between the orbit plane and the vector from the sun of any Earth-orbiting object [8], as shown in Figure 2-2 below. The beta angle varies between +90° and -90°, depending on the direction of the spacecraft. Viewing from the Sun, the beta angle is positive if the satellite is revolving counter clockwise and negative if the satellite is revolving clockwise. The satellite is exposed to more sunlight per orbit as beta angle increases, and eventually reaches constant sunlight exposure when beta angle is at 90 degrees. At high beta angle the satellite may get overheated if it is not properly controlled. As would be shown later in the Results and Discussion section for the analysis of the CubeSat for two beta angles, at 30 and 90 degrees, the heating rate for beta angle equaled 90 degrees was higher compared to the heating rate for beta angle equaled 30 degrees. On the other hand, the spacecraft would spend a shorter amount of time in sunlight and a longer amount of time in eclipse when the beta angle was small. The spacecraft might need heating to keep the electronic components within the various operating ranges. For small satellite that had a low power budget, such as the CubeSat, the power subsystem might not carry enough power to keep all the components warm. It was therefore best to keep the CubeSat's beta

angle at the range where it would receive a sufficient amount of time in sunlight and eclipse.

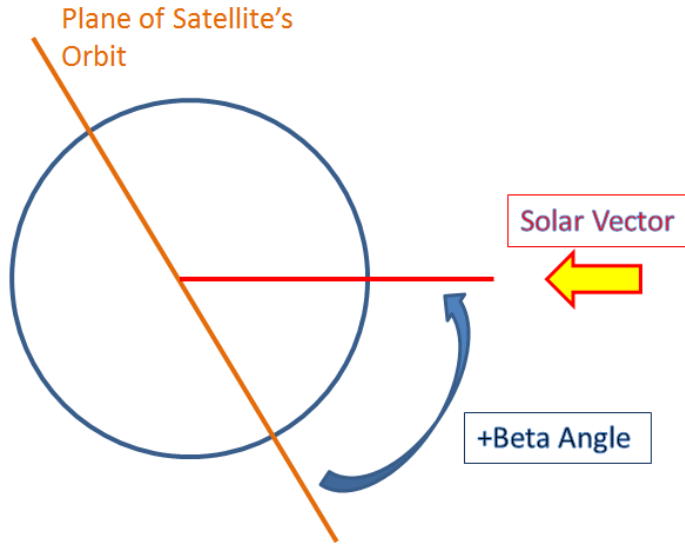


Figure 2-2 Beta Angle

Another important parameter for simulating the heating condition is the mission altitude. The orbital heating rate simulation was simplified by assuming that the CubeSat traveled in a circular orbit at 400 km altitude above the earth. Using the standard values for earth gravitational constant and radius, the orbit's semi-major axis a , orbital velocity v and period P were calculated as follows:

$$\mu_{Earth} = 3.986 * 10^5 \frac{km^3}{s^2} \quad (2.8)$$

$$R_{Earth} = 6378 \text{ km} \quad (2.9)$$

$$a_{mission} = R_{Earth} + h_{mission} = 6378 + 400 = 6778 \text{ km} \quad (2.10)$$

$$v = \sqrt{\frac{\mu_{Earth}}{a_{mission}}} = \sqrt{\frac{3.986*10^5}{6778}} = 7.67 \text{ km/s} \quad (2.11)$$

$$P = 2\pi \sqrt{\frac{a_{mission}^3}{\mu_{Earth}}} = 2\pi \sqrt{\frac{6778^3}{3.986 \times 10^5}} = 5535 \text{ seconds} \quad (2.12)$$

The number of orbits the satellite traveled in one day, or the mean motion (n) of the satellite was

$$n = \frac{86400}{P} = \frac{86400}{5431.01} = 15.9 \text{ revs/day} \quad (2.13)$$

Using the above equations, general orbital parameters various orbital heights were calculated and plotted in Figure 2-3 below. As could be seen from the figure, the orbital velocity varied from 7 to 8 km/s and the mean motion varied from 12 to 17 orbits per day for a general satellite in LEO.

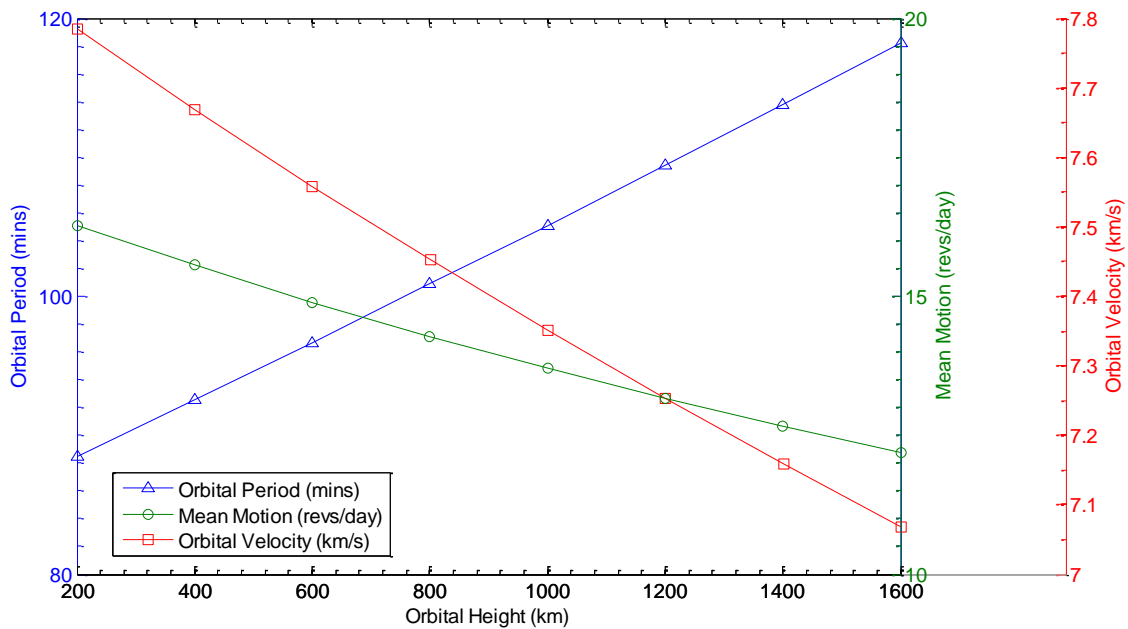


Figure 2-3 Orbital Parameters for Low Earth Orbit

The next step was to verify analytical results with the result from Thermal Desktop. The calculated period in the equation above was about the same as the result

shown in Figure 2-4. It should be noted that the calculation for orbital period depended only on the mission altitude and not the beta angle.

Figure 2-4 Thermal Desktop Orbit Input Options

Next, the angular radius at mission altitude was given by:

$$\rho = \sin^{-1} \left(\frac{R_{Earth}}{R_{Earth} + h_{mission}} \right) = \sin^{-1} \left(\frac{6378}{6378 + 400} \right) = 70.2 \text{ deg.} \quad (2.14)$$

The maximum time of eclipse (TE) and the time in sunlight (TS) were calculated as:

$$TE = \frac{2\rho}{360^\circ} P = \frac{2 \cdot 70.2^\circ}{360^\circ} 5553.6 = 2165.9 \text{ seconds} = 36.1 \text{ minutes} \quad (2.15)$$

$$TS = P - TE = 5553.6 - 2165.9 = 3387.7 \text{ seconds} = 56.5 \text{ minutes} \quad (2.16)$$

The time of eclipse and time in sunlight helped determine the expected thermal conditions of the spacecraft during these time intervals. For comparison, the orbital heating rate simulation was performed for three beta angles: (1) beta = 56.1°, (2) beta =

90° and (3) $\beta = 30^\circ$. The simulation for beta angle of 56.1 degrees was intended for the main mission in which further analysis was performed in subsequent sections. The simulation for beta angle of 90 and 30 degrees were provided for comparison purpose. Figure 2-5a showed the CubeSat in circular orbit for beta angle of 90 degrees. It could be seen that the CubeSat was always in direct sunlight at this beta angle, which meant that the heat flux was expected to be constant. For numerical simulation without the spinning effect, the result in a later section showed that the side directly facing the sun would receive a significantly higher heat flux compared to the other sides that were in eclipse. Figure 2-5b showed the circular orbit of the CubeSat for beta angle equaled 30 degrees. Both vehicle orientations were viewed from the sun perspective. As would be shown later in the Results and Discussions section, the heat flux in this case was not constant because the spacecraft would spend a portion of its period in eclipse.

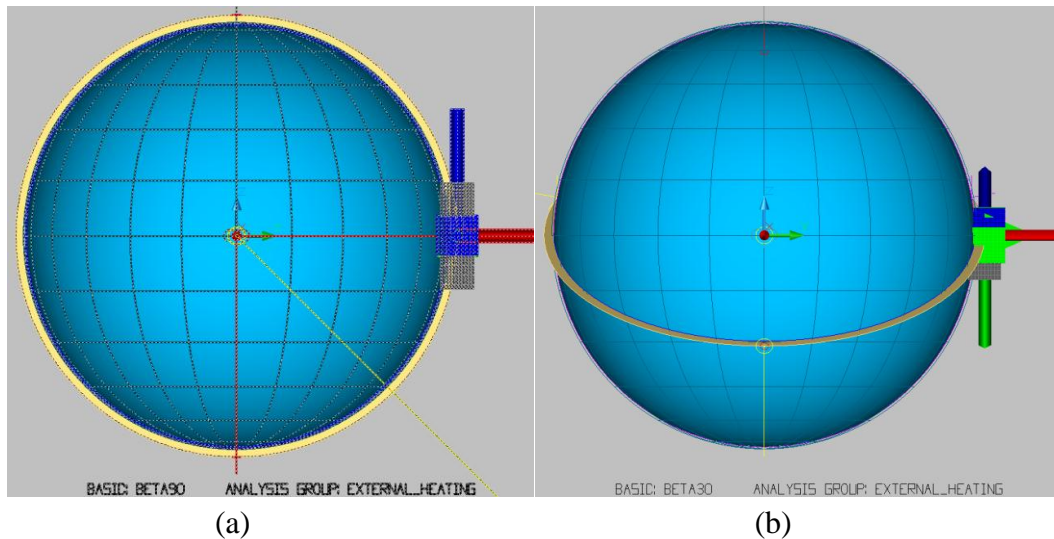


Figure 2-5(a) CubeSat Orbit for Beta Angle = 90°. **(b)** Beta Angle = 30°.

Another important parameter for mission analysis is the rate of decay, which is the rate at which the satellite de-orbits from the initial height before falling back and burning up in the atmosphere. This parameter helps determine the satellite lifetime and whether or not the satellite can operate for the duration of the mission requirement timeframe. The rate of decay is influenced by atmospheric drag and gravitational forces. The value of 2.2 has widely been used for the drag coefficient for spacecraft operating in LEO, although it is expected that this value tends to increase as the altitude decreases [9]. The Satellite ToolKit (STK) application from AGI was used for the mission analysis of the CubeSat. Using 400km for altitude, 56.1 degrees for beta angle and 2.2 for drag coefficient as the input parameters, STK calculated that the satellite has about a 7-month mission lifetime, as shown in Figure 2-6.

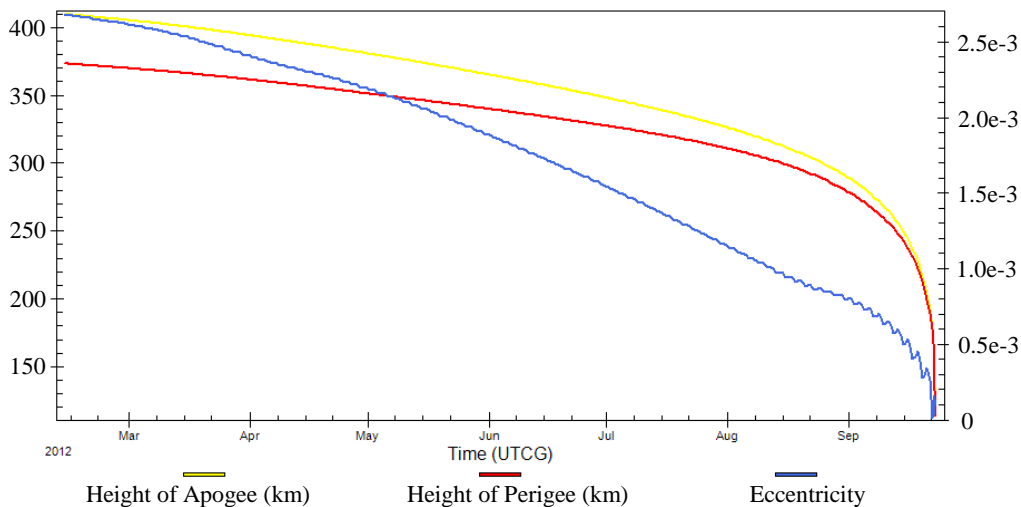


Figure 2-6 CubeSat Lifetime– Apogee, Perigee and Eccentricity Variation

Figure 2-6 showed the apogee, perigee, and eccentricity variation for the 400 km circular orbit satellite from the STK simulation. It could be seen that the rate of decay

was slow initially but quickly reached an abrupt end once the altitude of the satellite fell below 200 km. STK also has the capability of analyzing the heat transfer on the satellite but the appropriate license was not available for the analysis. An alternative approach, provided in the next section, was used in this thesis.

Chapter 3

CubeSat System Design and Power Budget Analysis

3.1 Subsystems Overview

Since the specifications for CubeSat standards were fairly limited in size and weight and that most CubeSats were only in space for a short duration due to budgetary cost and other constraints, this type of satellite utilized mostly passive control systems with relatively low power usage. The main subsystems of a typical CubeSat consisted of (1) hysteresis antenna for passive attitude control, (2) Pumpkin CubeSat Kit for structure, (3) radio communication system for communication, (4) battery and solar cells for power and (5) custom electrical hardware for power distribution, data handling, communication and control. An exploded view of the 3-D CAD model is shown in Figure 3-1.

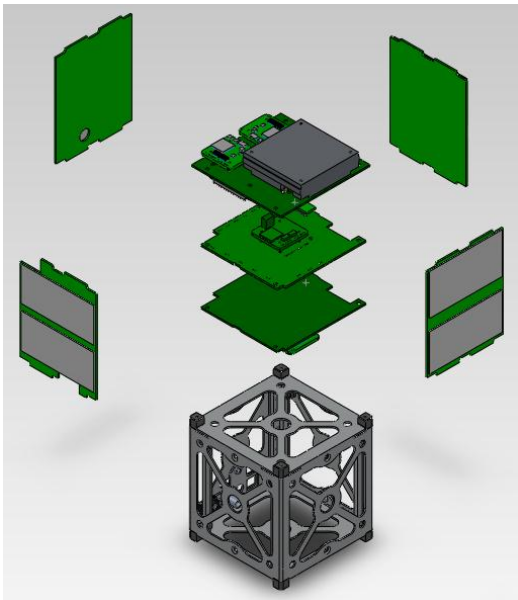


Figure 3-1 Example of a CubeSat Model – Exploded View

3.2 Attitude Control Subsystem

Upon ejection from the P-POD, the CubeSat rotated and spun arbitrarily in its designated orbit of around 400 km altitude. A passive attitude control subsystem using the hysteresis material and permanent magnet were used to dampen the potentially high rotational spin rate. The basic idea was that a passively controlled satellite would be aligned with the Earth's magnetic field through the use of a magnet installed on the satellite.

3.3 Structural Subsystem

Most CubeSat utilized a commercial-off-the-shelf (COTS) 6061 Aluminum frame structure from the Pumpkin CubeSat Kit. The advantages of using this structural kit were that (1) it adhered to the CubeSat Standards, (2) could easily be fitted into the standard Poly-PicoSatellite Orbital Deployer (P-POD) and (3) has been used successfully on other CubeSat projects from different university. With its proven success in withstanding the strong vibration environment during launch, this kit allowed the CubeSat designers to focus on other design aspects. Although the external interface was restricted by the CubeSat Standards, the internal configuration could vary depending on the payloads and mission objectives. As with any space vehicle, stress and vibration test were still necessary to quantify the structural integrity during transport and launch to ensure that the integrated components would be able to withstand the expected loads and vibrations. This topic, however, is beyond the scope of this thesis.

3.4 Communication Subsystems

Typically CubeSat designers have been using the amateur radio frequency for communication. With the objective of testing for the best communication systems for general purpose pico-satellite, the CubeSat had a total of three communication systems, which were (1) a HAM radio beacon, (2) OrbComm Q1000, and (3) Iridium 9602 modem.

The OrbComm Q1000 modem was a satellite-based communication system provided by the Orbcomm Communication Network. It had the operating temperature of $-40\text{ }^{\circ}\text{C}$ to $+85\text{ }^{\circ}\text{C}$. This system used 150 MHz for uplink and 138 MHz for downlink. Since this was a COTS product and the design parameters related to the thermal simulation were not known, the author decided to exclude this component from the thermal simulation. Through analytical and numerical solutions, it was assumed that if the average temperature inside the CubeSat was within the specified temperature limits of the components, then all the internal components were assumed to be operable. An actual experiment would be necessary to determine the operating temperature limits based on power input to validate and benchmark against numerical results.

3.5 Power and Electrical Subsystems (EPS)

As an overall passive system, the CubeSat used very little power. The electricity mainly came from an onboard battery pack and was recharged by using several arrays of high density solar cells installed on the external surface of the satellite. The electrical power was controlled and regulated by the main power distribution unit (MPDU). The

MPDU had a dedicated microcontroller to control the on and off states of the onboard components.

Table 3-1 shows a typical power budget of the CubeSat by estimating the approximate power consumption for the various subsystems for both active and passive states from different sources [6, 7]. The active state describes the satellite operating in the sun with most of the onboard subsystems turned on for communication and data handling. The standby state describes the operating state during eclipse, where only crucial components are powered.

Table 3-1 Power Budget for CubeSat

Component	Power (W)		Operating Limit
	Active	Standby	
Solar Panels	N/A	N/A	-150°C - 110°C
Battery	N/A	N/A	-10°C - 60°C
Chip 4	1.5	1.3	110°C Max.
Chip 1, 2 and 3	0.15	0.02	110°C Max.
Quake Q1000 (Active cycle = 0.5 second)	24	0.84	-40°C - 85°C
Iridium 9602 (active cycle = 0.5 second)	7.5	0.975	-40°C - 85°C

Chapter 4

Thermal Modeling Approach

4.1 External Analysis Approach

The radiation heating in the space environment could be either helpful or harmful to the CubeSat or spacecraft in general [7]. In some cases, the Sun's thermal energy and the Earth's albedo could help to warm electronic components to its normal operating temperature of about 20°C. In other cases, the heat generated from onboard computing combined with solar energy might cause overheating issues. Initial attempt to simultaneously simulate the external radiation and internal heat conduction was not successful because of the temporary limited software license available. The problem was de-coupled into two cases (1) internal heat conduction and radiation of the electronics using Icepak and (2) external heat radiation using Thermal Desktop. A combination of SolidWorks and AutoCAD were used to generate the computer model of the CubeSat. This decoupled analysis approach assumed that the external heating did not cause any changes to the internal environment and vice-versa. The assumption would be valid since the radiation effect was only significant if there was a high temperature differential between different objects. Otherwise it would cause about 5 to 10 percent error if the heat conduction from the external surface to internal surface of the case was significant.

The outer surface area of a CubeSat was usually covered on four sides with solar cells in order to generate as much power as possible. Since the solar cells behaved as a flat absorber, designing it on the sides reduced the heat load on the surface of the case

that did not face the sun. As mentioned in the previous chapter, the CubeSat spun as it orbited the Earth, which created a relieving effect that lowered the overall temperature as the surface continually absorbed heat from the sun and radiated heat to deep space. This was difficult to solve numerically for a steady state analysis. An alternative approach used in this thesis was to calculate the heat flux on each side individually and compute the average of the heat flux that could be uniformly applied to all sides.

Another point to note was that solar cells could be tricky to model thermally since a portion of the absorbed energy was converted to electricity and not heat [11]. For example, solar cells might convert 15% of the incident energy into electricity and another 40% into heat, leaving 45% of the energy reflected to nearby surfaces. If the value of absorptivity of 40% was used, then the amount of energy absorbed as heat was correct, but the reflected energy has an extra 15% of the incident energy. The solution to this was to ignore the 15% of the energy converted to electricity, and used 40% absorbed and 45% reflected energy. Table 4-1 provides the optical properties used in the analysis.

Table 4-1 Optical Properties

Description/Composition	α_s	ϵ^b	α_s/ϵ^b
Anodized Aluminum	0.14	0.84	0.17
Solar Cells	0.40	0.45	0.89
Tedlar White	0.39	0.87	0.448

4.2 Internal Analysis Approach

Ansys Icepak was used to perform the internal thermal simulation. The internal simulation focused on the main heat dissipation of each electrical component. The analyses were performed on the component level as well as for system level simulation.

For example, the BeagleBoard shown in Figure 4-1 that was typically used to build the CubeSat was performed separately on the component level. The system level simulation is discussed in details in the next chapter.

The BeagleBoard had the main heat source coming from the Texas Instrument's OMAP3530 720 MHz chip. All the connection interfaces, such as S-Video, Stereo In/Out, etc., were excluded from the analysis because the heat generated from these components was very small compare to the main chip. The BeagleBoard was designed for low powered application, and hence, did not require a heat sink. The PCB had an overall dimension of $76.2 \times 78.7 \times 1.6 \text{ mm}^3$ [1]. It was made up of multi-layered dielectric materials, such as FR4, and several layers of copper planes. From the BeagleBoard documentation [12], this board had 6 internal layers and the standard trace material of Cu-Pure was assumed for the simulation. The PCB board from BeagleBoard was a single overall layer board in which components were mounted on one side and the copper patterns were mounted and soldered on the opposite side. From the thermal modeling point of view, however, the PCB was treated as a homogeneous material with an orthotropic conductivity related to the copper layers in the substrate. The thermal physical properties used in this steady state heat conduction are provided in Table 5.1 below.

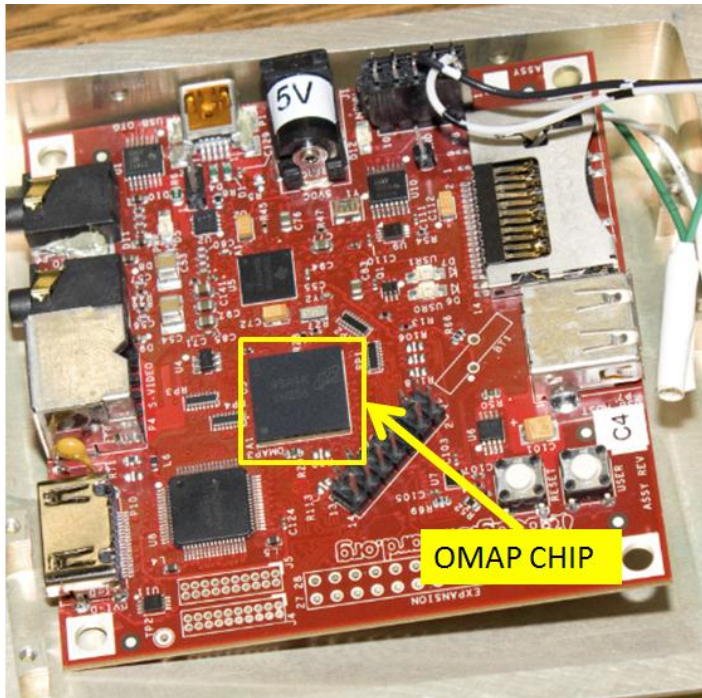


Figure 4-1 BeagleBoard Top Side Components

Table 4-2 Thermal Physical Properties

Description/Composition	Cond. [W/in/K]	Density [kg/in ³]	Cp [J/kg/K]
Aluminum (Alloy 2024-T6)	4.489*	0.04539	873.372*
FR4 2 oz Copper	0.44958	0	0
OMAP Chip	0	0.0327741	837.32

Note: * indicates property is temperature dependent.

The steady state heat conduction simulation assumed a constant heat load of 1.2 W applied on the OMAP chip. Figure 4-2 shows that 1.2 W heat load would produce a temperature of approximately 310K (37°C), which was within the safety limit of the electronic. This was expected because the BeagleBoard was designed for low powered applications. However, printed circuit boards generally endured high heat loads and it was difficult to provide heat dissipation capability for components such as voltage regulators. A solution to this was to use certain parts of the case, such as the back face,

for heat dissipation. A highly conductive material could be used to connect the hot component to the back face to reduce the heat load.

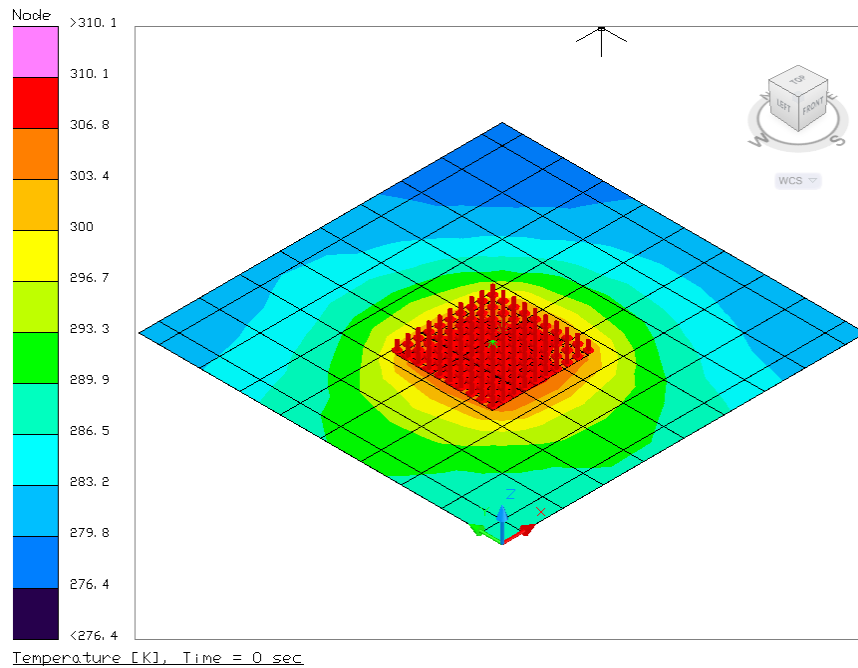


Figure 4-2 BeagleBoard Heat Conduction

An experiment was conducted to examine the validity of the numerical solution. The experiment consisted of applying a specified heat load to a copper block to simulate the heating condition of the microcontroller under full load. A temperature profile of 1.2 W applied to a 35 mm² copper block is shown in Figure 4-3. Two thermocouples were directly attached to the surface of the copper block to measure the temperature profiles, denoted as T_source1 and T_source2 in Figure 4-3. After about 40 minutes, the experimental model reached a maximum temperature of about 39°C. Comparing to the simulated model in Figure 4-2, the temperature difference between the two models was

about 2°C. This experiment showed that numerical method can be used for preliminary thermal design and analysis with reasonable accuracy.

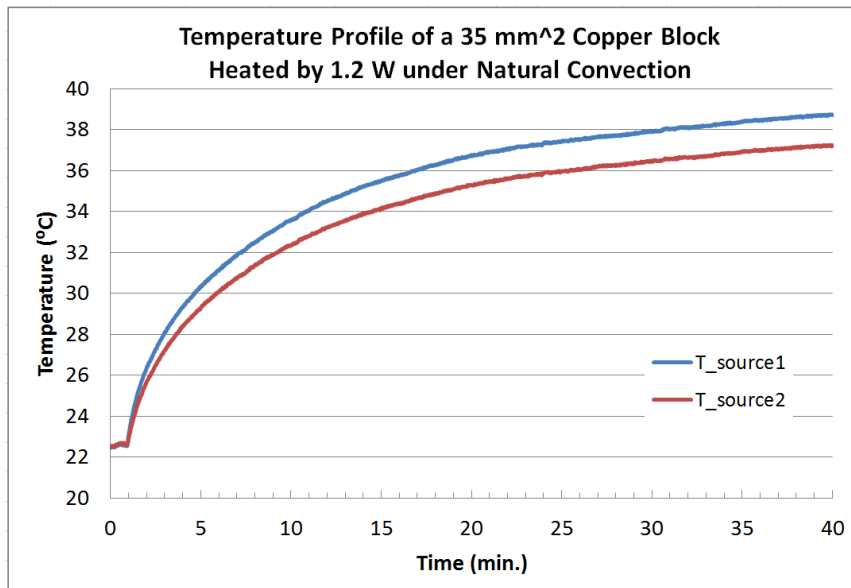


Figure 4-3 1.2 W Power Dissipation through CU Block Under Natural Convection

Chapter 5

Thermal Modeling Results and Discussion

5.1 External Analysis with Thermal Desktop

This section explains the orbital heating result for the external surfaces using Thermal Desktop. Figure 5-1 shows the setup of a CubeSat at 400 km circular orbit at 56.1° inclination angle. The external faces of the CubeSat were modeled as surfaces covered with solar panels. This simplification approach greatly reduced the complexity of the thermal model. The internal heat dissipation, as mentioned previously, was not taken into consideration for this external analysis. The thermo-optical properties of solar cells were selected based on the assumption that part of the incident energy is converted into electricity, part of it was reflected off the surface, and the rest was heating up the components. A more detailed setup is provided in Appendix B.

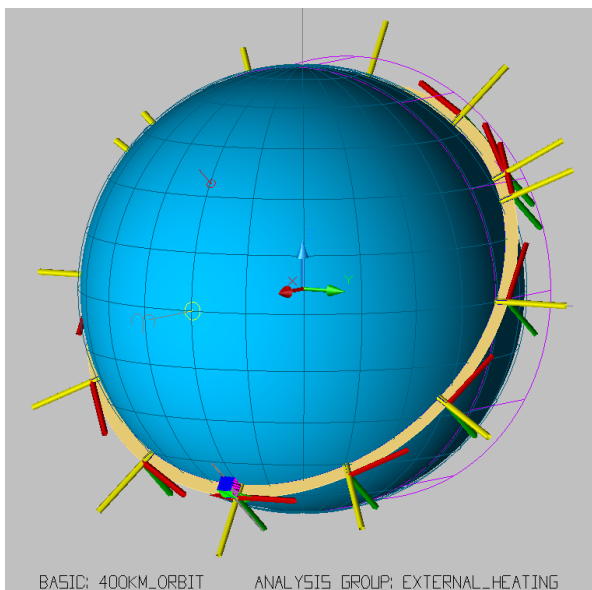


Figure 5-1 External Heating at 400 km Altitude

Figure 5-2 showed the external total absorbed heat flux profile of the CubeSat. As can be seen from the temperature profile, the heat flux on the side facing the sun was about twice the heat flux of the surrounding sides. Figure 5-3 showed the temperature variation on the sides by probing and monitoring points about the center of the front and right side faces. This plot showed that the heat flux on the sides of the CubeSat was about 100 W/m^2 during its period in the sun, and the heat flux was about 60 W/m^2 during its period in eclipse. It should be noted that the time periods during sunlight and eclipse, as shown in Figure 5-3, were congruent with the calculations in Chapter 2. Although the hysteresis antenna was included in the thermal model, it had negligible effect on the overall heat flux and could often be omitted.

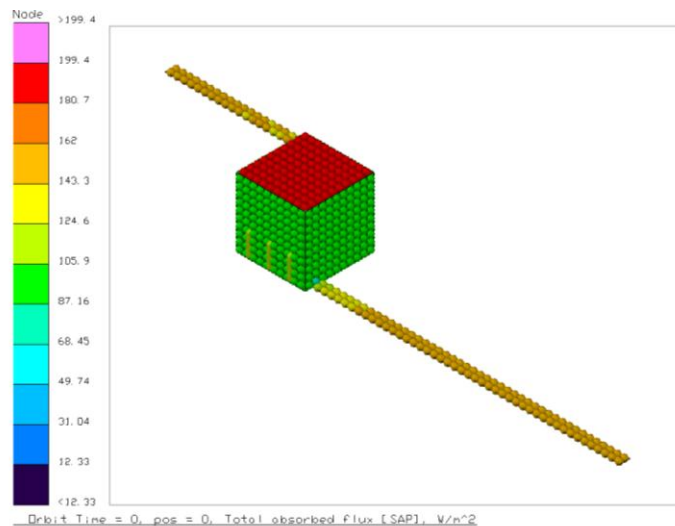


Figure 5-2 External Heat Flux

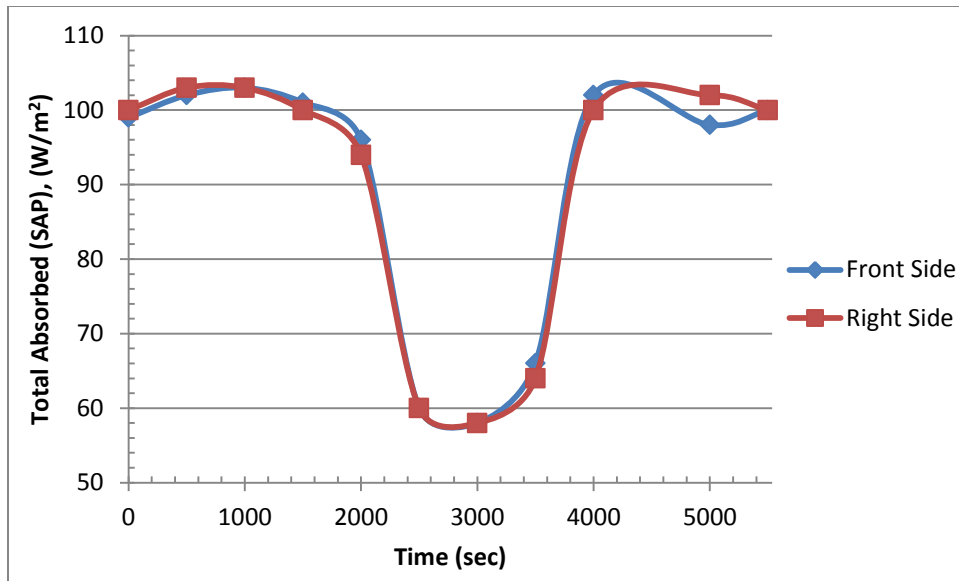


Figure 5-3 Total Absorbed Heat Flux for 400 km Altitude

5.2 Internal Simulation with Ansys Icepak

Ansys Icepak was used for modeling the internal components because the software has been well known for its ability to produce acceptable results in the electronics industry. The Icepak software used the Ansys Fluent solver as the back-end solver to numerically iterate values for the 3-D Navier-Stokes equations for the mass, momentum and energy using the finite volume technique. The simplified internal components of the CubeSat were created using Ansys Icepak. The simulation model was built based on the measured dimensions from the 3-D model of the Pumpkin CubeSat kit. The computational domain, also called “Cabinet” in Icepak, was created using the internal diameter of the CubeSat kit model. The additional objects, such as the PCB board or the chips, were added to the approximate coordinates on the CubeSat 3-D assembly model with approximate thermal physical and optical properties that closely

matched the model. The vacuum space environment was simulated by turning off the “flow” option in Icepak, and a very low thermal conductivity value was assigned to the ambient computation domain. The convergence criterion was set at $1e-7$ for the energy equation and an under-relaxation value of 0.7 was set for the momentum equation. The initial and boundary conditions were chosen to closely match the expected operating condition of the internal electronics. The model definition and mesh were passed to the Ansys FLUENT for computational fluid dynamic simulation, and the resulting data were post-processed using the ANSYS Icepak user interface.

The internal simulation was divided into two cases: (1) hot case and (2) cold case. The hot case analysis represented the satellite position in direct sunlight, and the cold case analysis represented the satellite position in eclipse. Figure 5-4 shows the temperature distribution of various components for the hot case analysis.

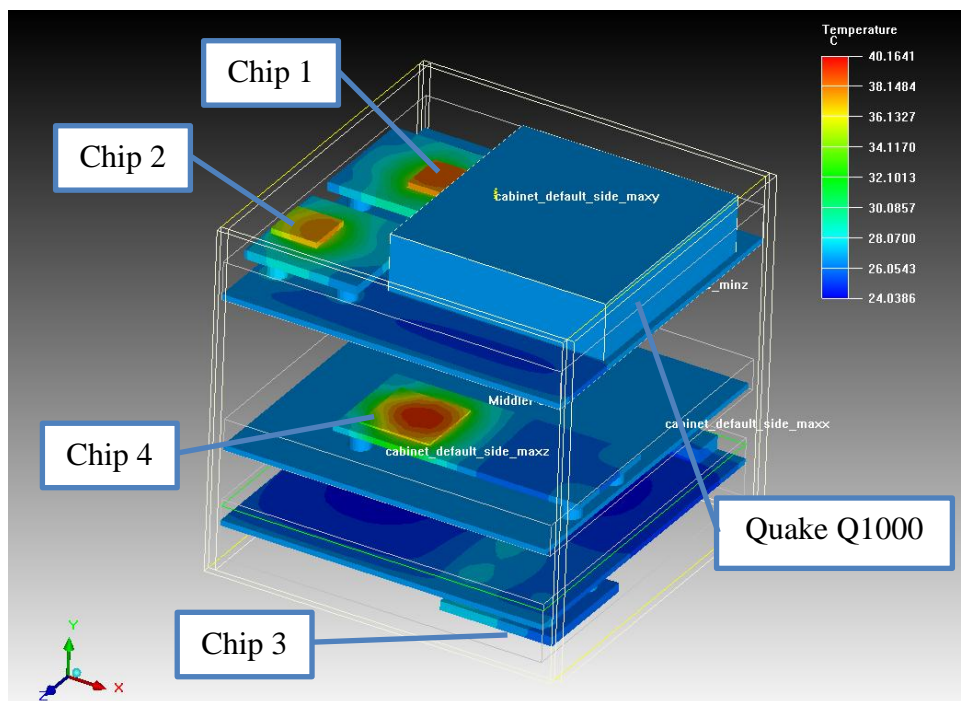


Figure 5-4 CubeSat Temperature Profile – Hot Case Analysis

Even though the same power of 0.15 W was applied to Chip 1 through 3, Figure 5-4 shows that the temperatures of the components varied slightly depending on the location of the chip relative to the other heating sources. The Quake Q1000 is a propriety commercial product that does not disclose the power consumption of the internal components. Since this product has an operating temperature range from -40°C to $+85^{\circ}\text{C}$ and the CubeSat internal environment is within the range, it was assumed that the Quake Q1000 would be fully functional without further analysis. To study what effect it had on the other component, the overall system of the Quake Q1000 was modeled as a radiating block with the surface temperature assumed to be at 40°C . This caused the temperature on Chip 1 to be slightly higher than that of Chip 2. The temperature rise of the overall system was about 15°C .

Figure 5-5 shows the temperature profile of the internal components for the “cold case” simulation. With the initial operating temperature of -75°C , the temperature rise for this case was about 57°C , which was almost 4 times higher comparing to the “hot case”. The variation of temperature between Chip 1 and Chip 2 was much higher than the “hot case”. The simulation for this case represented a worse case analysis that might not accurately predict the temperature distribution of a real case. For example, as the CubeSat orbits from direct sunlight to eclipse area, the temperatures of the component are higher and slowly cooling down, which is not possible to model using the steady state method.

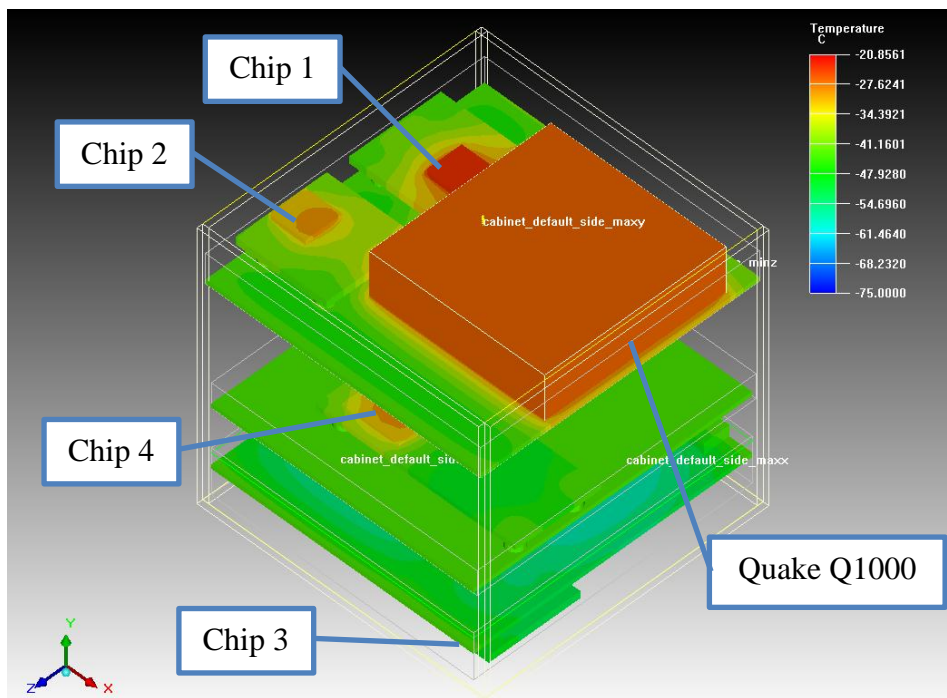


Figure 5-5 CubeSat Temperature Profile – Cold Case Analysis

Table 5-1 shows the tabulated temperatures of the main components for both the “hot case” and the “cold case” analysis. As mentioned previously the same power

consumption was used for both cases, while an actual experiment might have different power settings for different cases. When the CubeSat was in direct sunlight and the solar panels were charging the battery, the electrical components were more likely to operate at full power compared to the eclipse case. Based on the “cold case” analysis, an electric tape heater might be necessary to keep the internal components within the safety limits while the CubeSat was in the eclipse region.

Table 5-1 Component Temperatures

Component	Power (W)	“Hot Case” Temperature (°C)	“Cold Case” Temperature (°C)
Chip 1	0.15	39.6	-34.7
Chip 2	0.15	39.2	-20.7
Chip 3	0.15	38.4	-28.6
Chip 4	0.2	40.2	-27.3
Quake Q1000	N/A	40 [reference temp.]	40 [reference temp.]

Chapter 6

Design of Experiments Simulation

The previous chapter discussed the analysis of a CubeSat operating at a specific altitude and orbit. This chapter explores how different design parameters, such as inclination angle or altitude, affect the thermal performance of the CubeSat. For example, by adding the two solar panels on the sides of the CubeSat to collect more solar energy, as shown in Figure 6-1, the orbital heating was slightly higher compared to only having solar panels on the sides. The view displayed the total absorbed flux using the sum of all heating rate sources (solar, albedo, and planet shine). Unlike the uniform heat flux on the surrounding faces, the top and bottom surfaces with the solar cells attached had a non-uniform behavior. This was because these two sides experienced some radiation from the back of the solar cells hitting the top and bottom surfaces of the case, and vice versa.

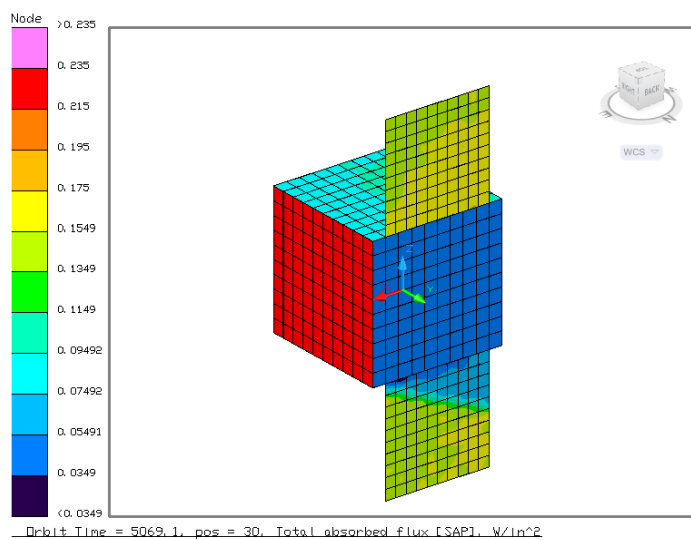


Figure 6-1 CubeSat Total Absorbed Flux

Another parameter that influences the thermal performance of the CubeSat is the beta angle. To study the effect of beta angle on the spacecraft, two simulations were performed for beta angles of 90° and 30°, respectively. The spinning effect was not included in this simulation; this allowed the author to study how the beta angle affects the thermal performance without the bias influence from other factors. Figure 6-2 shows the orbital heat flux for the 90° beta angle. Each line on the graph represents a node on each surface of the spacecraft. As expected, the heat flux remained constant throughout its period because its position and orientation relative to the sun did not change. The heat flux for 30° beta angle, however, did change with time. This was because a portion of its time was spent in eclipsed while the rest of the time it faced sunlight. The changes in orbit cycles also resulted in changes in thermal cycles.

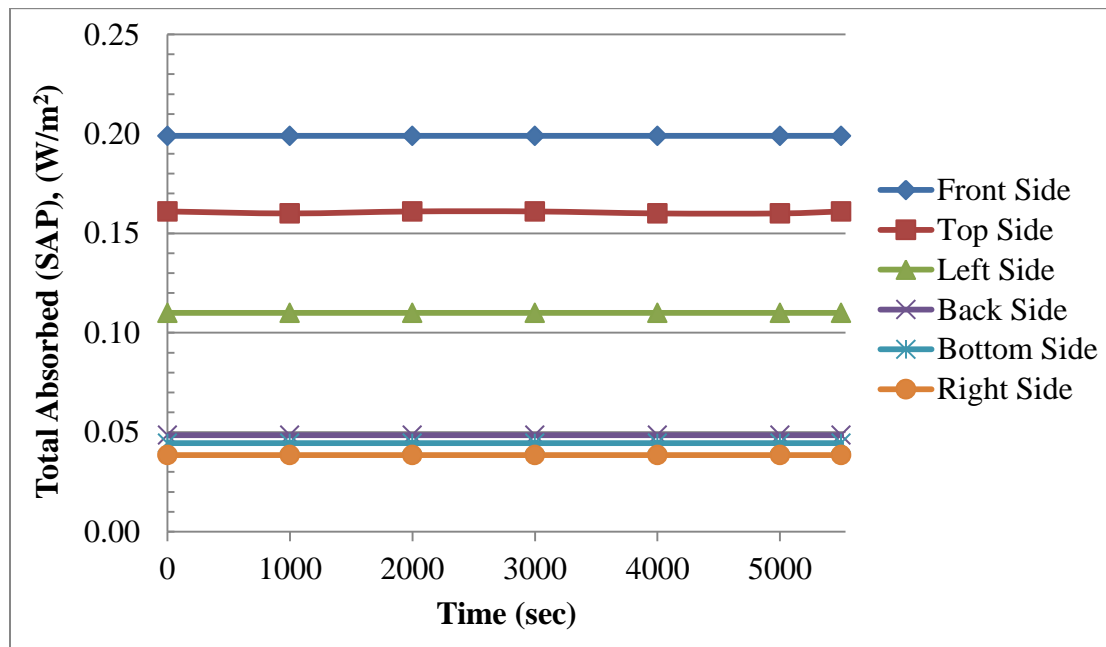


Figure 6-2 Total Absorbed Heat Flux for Beta Angle = 90°

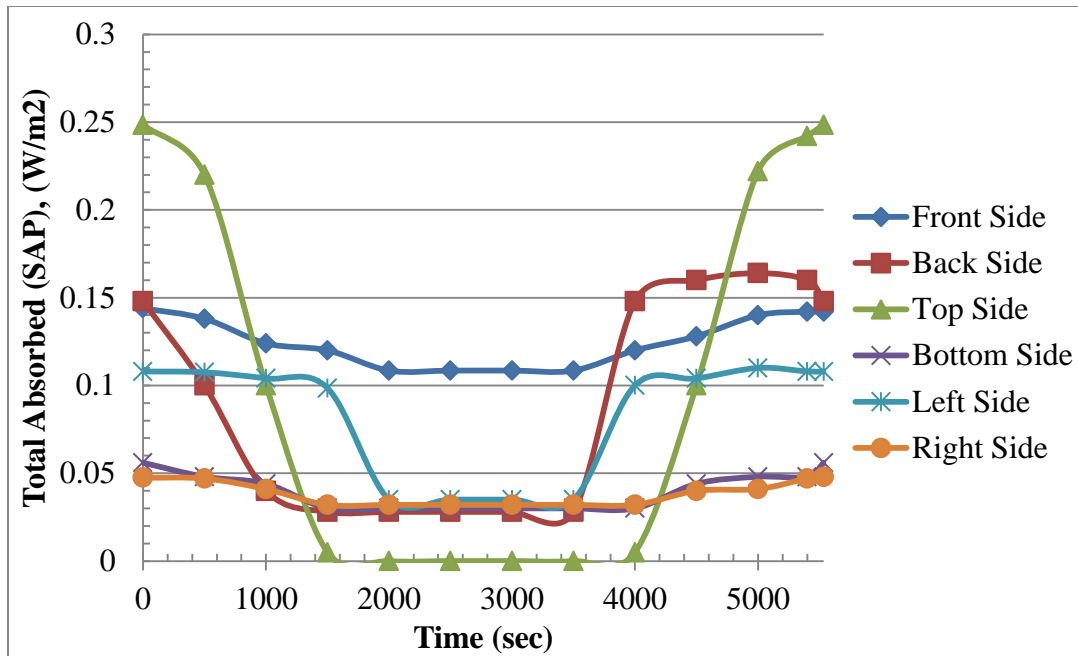


Figure 6-3 Total Absorbed Heat Flux for Beta Angle = 30°

As can be seen from Figure 6-3, the total absorbed heat flux remained constant from approximately 1,700 to 3,800 seconds. During these 2,100 seconds, or 35 minutes, the CubeSat was facing the back side of the Earth and did not see the heat flux from the sun. This estimate from the graph was about the same as the calculated value using the equations provided in the Orbital Mechanics section. The graph showed that the CubeSat's heat flux increased and/or decreased in periodic pattern with respect to the position of the spacecraft in orbit. The thermal analyst could use this information to design the thermal control system that could meet both operating conditions. This information was used to calculate the required energy during eclipse, and the power generated using solar cells during sunlight. Combining all the information could result in a design that was optimized for mass as well as power. This chapter showed that the beta angle had a major influence on the external heating rate of a satellite in LEO.

Chapter 7

Conclusions and Future Work

In this thesis we analyzed the thermal performance of the nano-satellite in the Low Earth Orbit at 300 and 400 km altitude. High fidelity level models were used to predict the temperature variations on the external body and the internal electrical components. The components did not overheat in the hot case simulation because onboard components were mostly low-power devices. Looking ahead, the electronics will likely continue to shrink while adding more power and functionality. It is expected that future designs of CubeSats will include high-powered components to accommodate more sophisticated missions. Thermal control will be necessary to ensure system reliability. From the thermal analysis aspect, thermal control options available for miniature size spacecraft are limited. Active thermal control systems would take up too much space as well as electrical power. On the other hand, a passive thermal control system might not be adequate for certain operating conditions of the spacecraft. Therefore it is important to continually update the thermal model as the design changes take place to determine the best possible thermal control option. This process would make sure that the system functions properly and that the overall system is well optimized for mass and power budgets.

Although numerical simulation can be used as a guide for designing the CubeSat, actual thermal testing of the system is still needed to ensure that the system can operate without failure. Current numerical simulation methods are created based on a simplified

model of the system and should only be used to compliment testing because numerical model, due to software limitations, cannot simulate all physical conditions correctly. For example, the Ansys Icepak software used for internal electronic simulation was designed for the earth environment and lack the option to simulate the vacuum environment of space. The space environment was simulated by switching off all the flow parameters and assigned a very low thermal conductivity for the surrounding ambient domain, simulating a model at very high altitude. The spinning effect of the satellite was not simulated in the steady state analysis. It was expected that as the satellite would spin while it traveled in its designated orbit, the heat exchange between the hot surface and the cold deep space reduced the overall maximum temperature of the vehicle. Another limiting factor in thermal modeling was that some manufacturers did not provide sufficient data to control a numerical model. These components were omitted in the numerical model, but actual testing would provide valuable data on the temperature distribution of the overall system.

The aluminum case structure that is typically used for building CubeSats can be optimized to reduce weight, while still maintaining the structural integrity. Since the CubeSat weight specification is limited to 1 kg, further structural study is needed to optimize for the weight. The structural optimization can be couple with thermal optimization to determine the best design.

The key issues of thermal design are performance, reliability and cost. As electronic devices become more complicated and practical applications require more

power, thermal analysis using CFD tools become indispensable for the design engineers. With sufficient funding, university students can gain valuable hands-on experience building the CubeSat model and launching it into space. The CubeSat model can be used to effectively conduct scientific experiments.

References

- [1] Nugent, R., Munakata, R., Chin, A., Coelho, R., & Puig-Suari, J. "The CubeSat: The Picasatellite Standard for Research and Education". *American Institute of Aeronautics and Astronautics*, 2008.
- [2] Herrell, L.M.; , "Access to Space for Technology Validation Missions: A Practical Guide," *Aerospace Conference, 2007 IEEE* , vol., no., pp.1-8, 3-10 March 2007
doi: 10.1109/AERO.2007.352787
- [3] Jacques, Lionel. *Thermal Design of the OUFTI-1 NanoSatellite*. Master Thesis, University of Liege, 2009.
- [4] Gadalla, M. "Prediction of temperature variation in a rotating spacecraft in space environment." *Applied Thermal Engineering*, Vol. 25, No. 14-15, 17 Feb. 2005, pp. 2379-2397, 2005.
- [5] Incropera, F, D DeWitt, T Bergman, and A Lavine. *Fundamentals of Heat and Mass Transfer*. New York: John Wiley & Sons, 2006.
- [6] Larson, W., and J. Wertz. *Space Mission Analysis and Design*. New York: Microcosm Press and Springer, 1999.
- [7] Fortescue, P., G. Swinerd, and J. Stark. *Spacecraft Systems Engineering*. 4th. Chichester, West Sussex: John Wiley & Sons, Ltd, 2011.
- [8] K&K Associates. "Earth's Thermal Environment". *Thermal Environments JPL D-8160*, URL:<http://www.tak2000.com/data/planets/earth.htm> [cited 1 May 2010].
- [9] Cook, G. E. (1965). "Satellite drag coefficients". *Planet Space Science*, Vol. 13, No. 10, 27 May 1965, pp. 929-946.
- [10] Rotteveel, J., & Bonnema, A. "Thermal Control Issues for Nano- and Picosatellites". International Astronautical Federation, 2006.
- [11] C&R Technologies, Inc. *Thermal Desktop User's Manual, Version 5.2*. Littleton: Cullimore and Ring Technologies, Inc., 2008.
- [12] BeagleBoard. *BeagleBoard System Reference Manual, Rev C4*, Richardson: BeagleBoard.org, 2009.

APPENDIX A – STK Setup

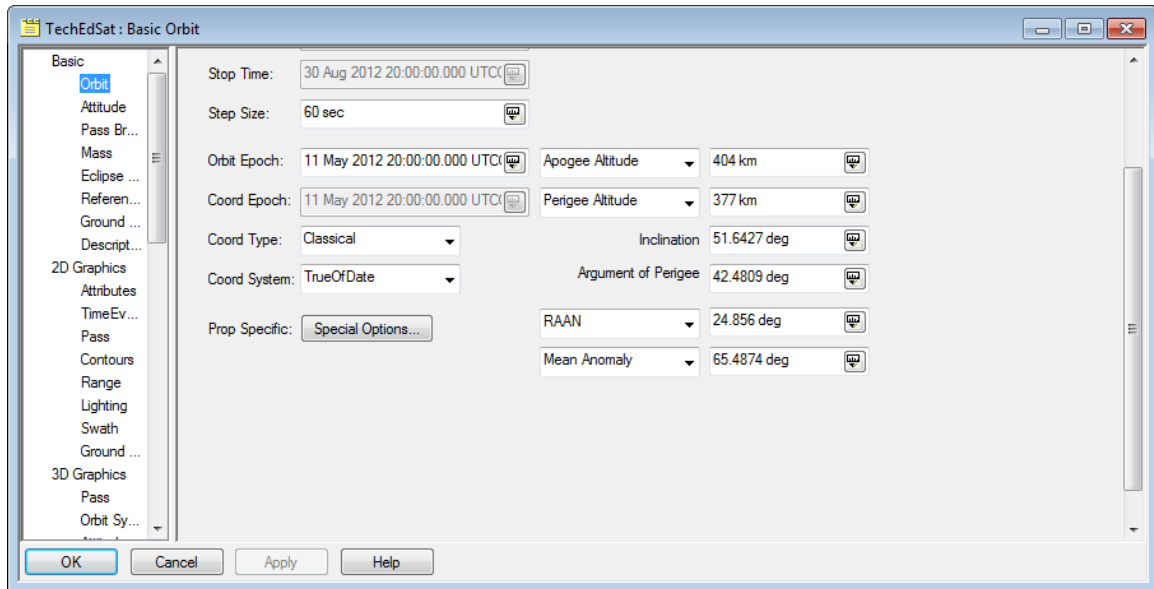


Figure A-1 Satellite Orbit Setup in STK

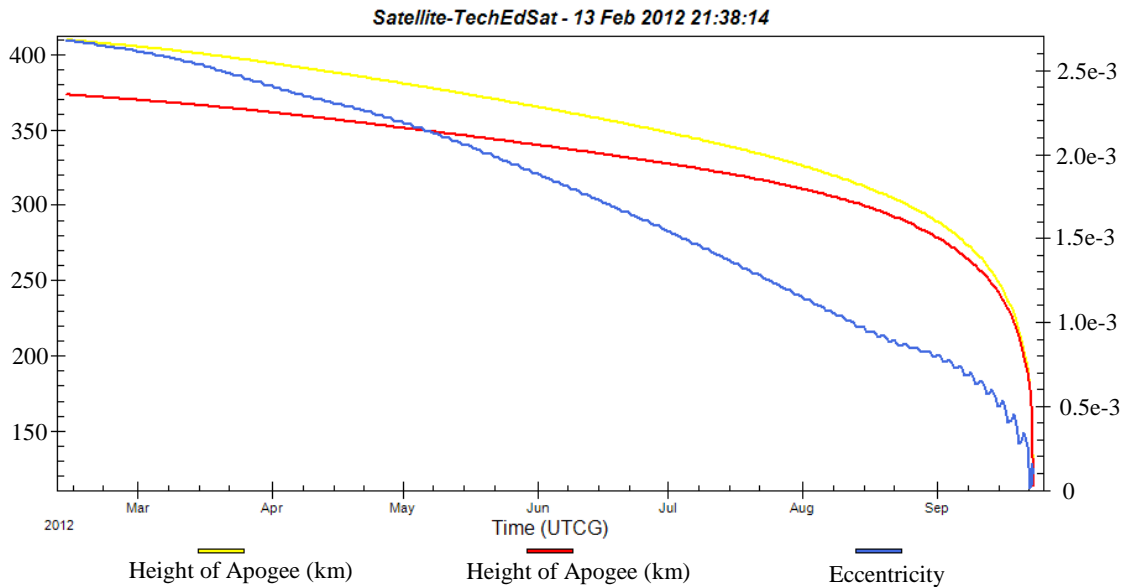
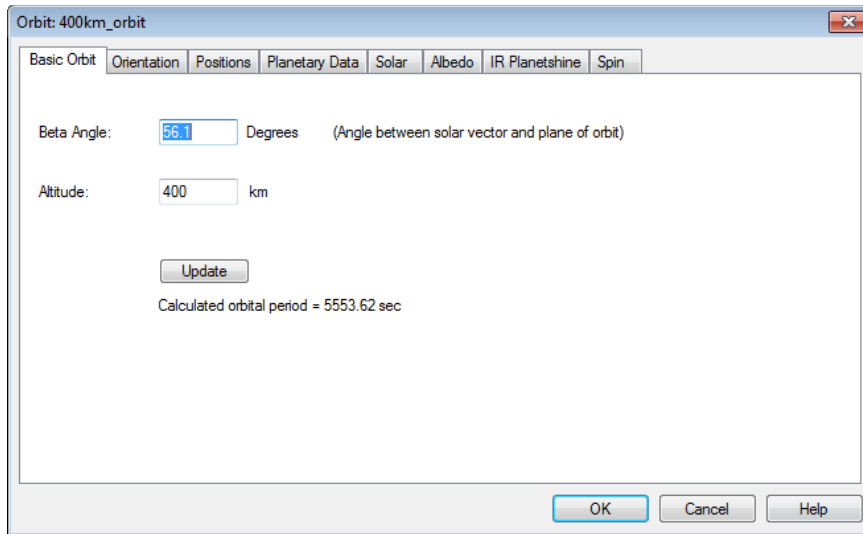


Figure A-2 CubeSat Lifetime – Apogee, Perigee and Eccentricity Variation

APPENDIX B – Thermal Desktop Setup Guide

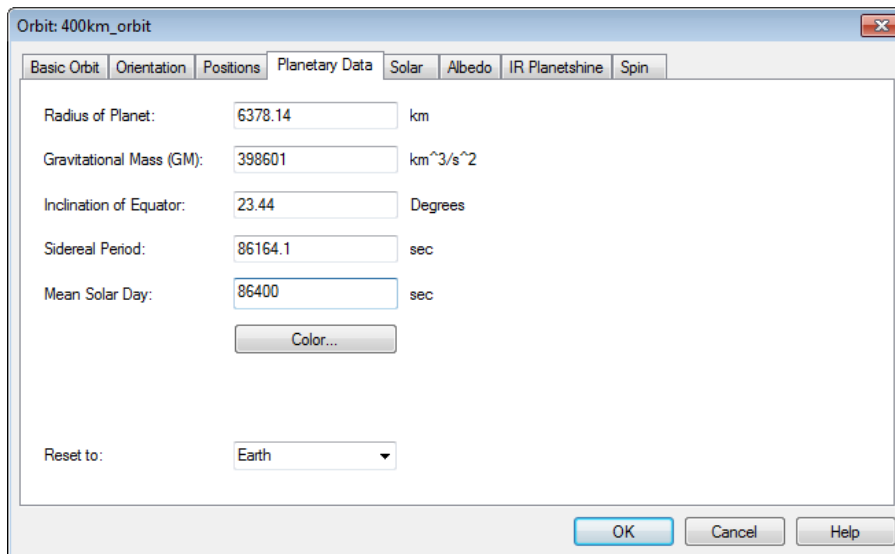
Thermal Desktop from C&R Technologies was used for the external orbital heating rate. It allows heat transfer calculations to be performed at any specified mission altitude. Below are some general steps used to set up the external analysis.

1. Enter the information for the beta angle and mission altitude.



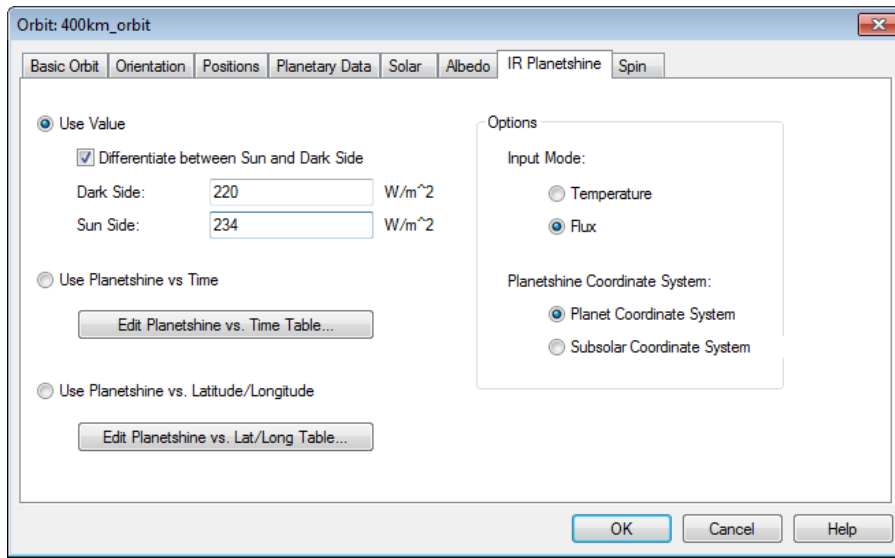
The screenshot shows the 'Orbit: 400km_orbit' dialog box with the 'Basic Orbit' tab selected. The 'Beta Angle' is set to 56.1 Degrees, with a note '(Angle between solar vector and plane of orbit)'. The 'Altitude' is set to 400 km. An 'Update' button is present, and the 'Calculated orbital period' is displayed as 5553.62 sec. The dialog has 'OK', 'Cancel', and 'Help' buttons at the bottom.

2. The orientation and positions of the satellite can be changed under the Orientation and Positions tabs. For CubeSat operating in LEO, the Earth parameters were used under Planetary Data tab.

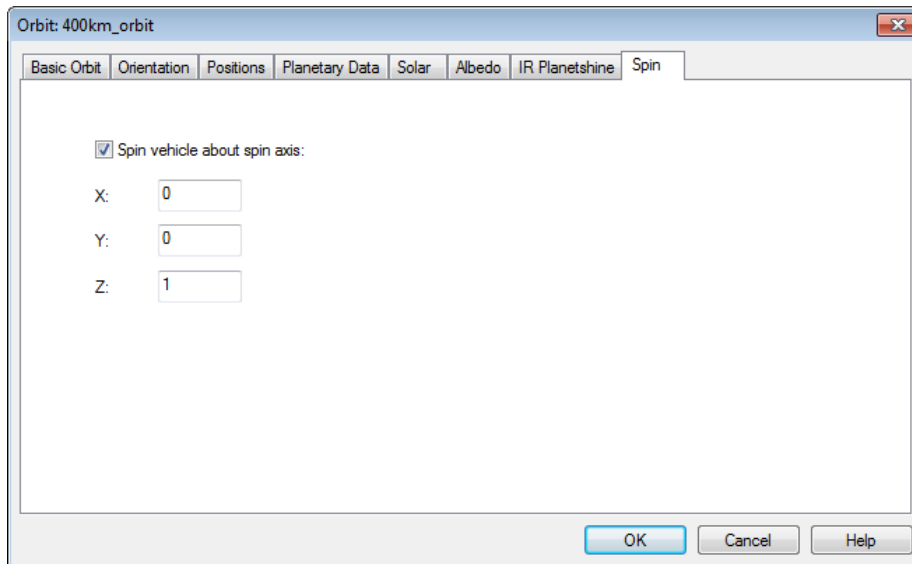


The screenshot shows the 'Orbit: 400km_orbit' dialog box with the 'Planetary Data' tab selected. The parameters are: Radius of Planet: 6378.14 km; Gravitational Mass (GM): 398601 km³/s²; Inclination of Equator: 23.44 Degrees; Sidereal Period: 86164.1 sec; Mean Solar Day: 86400 sec. There is a 'Color...' button and a 'Reset to:' dropdown menu set to 'Earth'. The dialog has 'OK', 'Cancel', and 'Help' buttons at the bottom.

3. Next, enter the heat flux values for the hot case and cold case.



4. If the satellite spins as it orbit the earth, the option can be set under Spin tab.



5. The last step is to double check the thermal and optical properties for the simulation. It should be noted that not all the optical properties shown in the figure below were included in the actual simulation.

